Quantum force induced on a partition wall in a harmonic potential

2009 J. Phys. A: Math. Theor. 42 475301

(http://iopscience.iop.org/1751-8121/42/47/475301)

J. Phys. A: Math. Theor. **42** (2009) 475301 (19pp) doi:10.1088/1751-8113/42/47/475301

Quantum force induced on a partition wall in a harmonic potential

T Fülöp[1] **and I Tsutsui**[2]

[1] Montavid Thermodynamic Research Group, Igmándi u. 26. fsz. 4, 1112 Budapest, Hungary
[2] Institute of Particle and Nuclear Studies, High Energy Accelerator Research Organization (KEK), Tsukuba 305-0801, Japan

E-mail: tamas.fulop@gmail.com and izumi.tsutsui@kek.jp

Received 16 June 2009, in final form 24 September 2009
Published 29 October 2009
Online at stacks.iop.org/JPhysA/42/475301

Abstract
Boundary effects in quantum mechanics are examined by considering a partition wall inserted at the centre of a harmonic oscillator system. We put an equal number of particles on both sides of the impenetrable wall keeping the system under finite temperatures. When the wall admits distinct boundary conditions on the two sides, then a net force is induced on the wall. We study the temperature behaviour of the induced force both analytically and numerically under the combination of the Dirichlet and the Neumann conditions, and determine its scaling property for two statistical cases of the particles: fermions and bosons. We find that the force has a nonvanishing limit at zero temperature $T = 0$ and exhibits scalings characteristic to the statistics of the particles. We also see that for higher temperatures the force decreases according to $1/\sqrt{T}$, in sharp contrast to the case of the infinite potential well where it diverges according to $\sqrt{T}$. The results suggest that, if such a nontrivial partition wall can be realized, it may be used as a probe to examine the profile of the potentials and the statistics of the particles involved.

PACS numbers: 03.65.−w, 02.30.Mv, 02.30.Tb, 02.60.−x, 02.60.Lj, 05.30.−d, 05.30.Jp, 05.30.Fk

1. Introduction

Quantum systems are often delineated by modelling their classical counterparts—in fact, it is a standard practice that we define a system in quantum mechanics through the procedure called 'quantization', which amounts to replacing functions of phase space in classical mechanics by appropriate operators based on commutation relations. However, this quantization procedure does not necessarily provide a unique quantum system to a given classical system, with the familiar example being the ordering ambiguity of operators. Nontrivial topology of the

classical configuration space furnishes an additional ambiguity in the quantum system, which is exemplified by a particle moving on a circle where a multiple of windings are allowed for transitions. In particle physics, the same topological effect is known to be responsible for the infinite vacua structure which causes the strong CP violation (see, e.g., [1]).

Another source of ambiguity, which is less recognized and yet physically more tangible than the aforementioned ones, lies in the choice of boundary conditions imposed on quantum states [2–4]. A prime example of this may be found in a particle system with an impenetrable wall, where one has a variety of boundary conditions to choose, say, from Dirichlet to Neumann or anything in between. These boundary conditions represent different physical properties of the wall which are missing in the classical description, and can lead to novel effects in the quantum system [5]. A further example is provided by a singular point on a line, which serves as a source for a number of interesting properties, including supersymmetry and Berry phase [6–8]. The importance of boundary conditions in quantum mechanics becomes evident if we recall the rudimentary fact that a different choice of boundary conditions yields a different spectrum. The fact that the physical properties of quantum dots depend heavily on the boundary conditions will also be worth mentioning.

In order to provide a simple setup where the boundary effects can be observed directly, in our previous work [9] we presented a case study of the induced pressure, or statistical quantum force, which emerges on an impenetrable partition wall inserted at the centre of an infinite potential well, when the wall is assumed to realize a nontrivial set of boundary conditions: the Dirichlet condition on one side and the Neumann on the other. We will not delve into here how such a partition can actually be manufactured as a device, but only mention that walls admitting generic boundary conditions including Dirichlet and Neumann can be realized by a combination of square-well potentials in the vanishing limit of their widths [5]. When two such walls, one with Dirichlet and the other with Neumann, are 'glued together' within a narrow distance, then it will serve as our partition effectively under a scale significantly larger than the distance. In more formal terms, our partition is a special example of the general ($U(2)$ family of) point singularities allowed quantum mechanically on a line, whose realizations by scaled families of regular potentials have been studied extensively [4].

Once the partition wall is realized and placed in the well separating the same number N of particles on its two sides, under the finite temperature T we expect that the wall is pushed from the two sides by the particles in motion. Now, the point is that the different boundary conditions imposed at the partition cause different energy levels and, accordingly, different statistical distributions of particles in the levels between the two half wells, yielding a net force ΔF on the wall. In [9] we investigated the behaviour of the force ΔF as a function of T, and examined how it scales with particle number N for the two kinds of particle statistics, the Bose–Einstein statistics and the Fermi–Dirac statistics. There we have found that the force ΔF has a finite limit at zero temperature $T = 0$ which scales as N for bosons and as N^2 for fermions, and that it has a minimum before it diverges as $\sqrt{T}$ for the high temperature limit $T \to \infty$.

This raised a natural question if these results are specific to the potential used in the analysis, and if so how. In the present paper, we attempt to answer this by considering the same partition wall placed in a different potential, namely the harmonic oscillator potential (see figure 1). One of the reasons for the harmonic potential is that, unlike the infinite well potential, it stretches infinitely for higher energies and shares a feature with potentials which are often used to describe actual physical systems. Another reason is that, on account of its technical simplicity which we also exploit here, the harmonic potential itself is widely used in various physical contexts including confinement of particles in a narrow region. Again, as illustrated in figure 2, we consider both bosonic and fermionic cases for particle statistics,

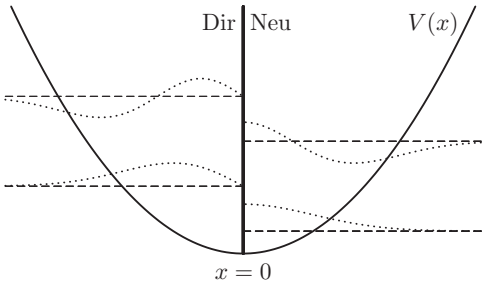

Figure 1. The eigenfunctions and eigenvalues under the harmonic potential $V(x) = \frac{m\omega^2}{2}x^2$ with a partition at the centre. If the partition admits the Dirichlet ($\psi = 0$) and the Neumann ($\psi' = 0$) boundary conditions on the left and on the right, respectively, the eigenstates (the lowest two are shown in both half lines) possess different energy levels. When the same number N of particles are introduced in each of the half lines, these level differences give rise to a net force on the partition.

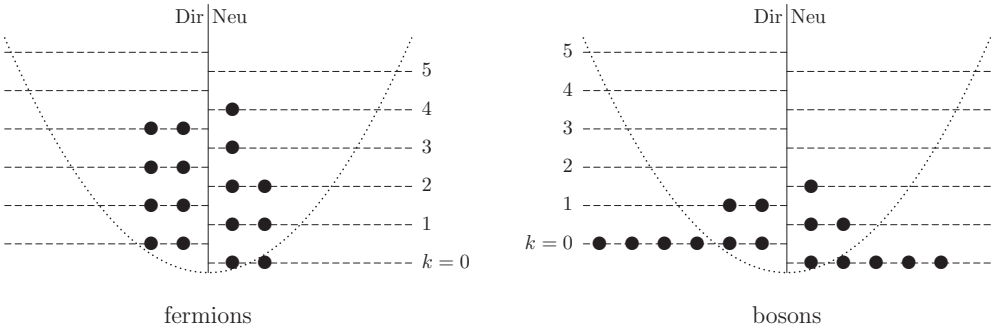

Figure 2. Illustration of particle distributions over the levels in the two half lines at a low temperature. The force related to each level differs on the two sides of the partition and induces a non-vanishing net force on the partition, which is dependent on temperature as well as on the particle statistics.

and the number N of particles is regarded as large but not macroscopically large (to ensure its possible relevance to nano devices). We derive analytic approximate formulae for the force in the low-, medium- and high-temperature regimes separately, which are found to be reasonably good to reproduce the numerical results obtained for $N = 100$. Note that, in actual realizations, our one-dimensional system can be regarded as a model of an axis in three dimensions perpendicular to the surface of the partition which attracts the particles by the harmonic potential.

Our analysis then shows that, in contrast to the infinite well case, the force ΔF on the wall decreases as $1/\sqrt{T}$ as the temperature increases in the high-temperature regime, and eventually vanishes in the limit $T \to \infty$. This is the case for both bosons and fermions, and the force is of the order of N. For the low-temperature regime, the zero temperature limit of the force is of the order of N for bosons as in the potential well case, but for fermions it is of the order of $\sqrt{N}$ in contrast to N^2 obtained in the potential well. We also find that, unlike the infinite well case, no minimal point of the net force is found in the medium-temperature regime irrespective of the statistics of the particles. Implications of these results, combined with the previous ones, will be discussed in the text.

This paper is organized as follows. In section 2 we define the model and provide our scheme of analytical approximation for the induced force at arbitrary finite temperatures. In section 3, we present our analysis in detail for the high-temperature regime as well as the numerical results obtained. Section 4 is devoted to the analysis of the low-temperature regime, where we employ independent approaches for the fermionic and bosonic cases. Section 5 discusses the medium-temperature regime where we also seek to interpolate the other two temperature regimes. Finally, we present our conclusion and discussions in section 6.

2. Definition and basic properties of the system

In this section, we first define the system mentioned earlier and introduce some notations convenient for the description of the system. With these, we present our basis of evaluating the induced force on the wall, and provide our scheme of analytical approximation used later.

2.1. The eigenstates and distributions at finite temperatures

To begin with, we recall the basic result of a harmonic oscillator system. For a particle moving on a line under the harmonic potential $V(x) = \frac{m\omega^2}{2}x^2$, the normalized energy eigenfunctions $\phi_l(x)$ and the corresponding energy eigenvalues $\mathcal{E}_l$ obeying the equations

$$H\phi_l(x) = \mathcal{E}_l\,\phi_l(x), \qquad H = -\frac{\hbar^2}{2m}\frac{d^2}{dx^2} + \frac{m\omega^2}{2}x^2 \tag{1}$$

are given by

$$\phi_l(x) = \frac{1}{\sqrt{a}}\frac{1}{\sqrt[4]{\pi}}\frac{1}{\sqrt{2^l l!}}\,\mathrm{H}_l\Big(\frac{x}{a}\Big)\,\mathrm{e}^{-\frac{x^2}{2a^2}}, \qquad \mathcal{E}_l = \frac{\mathcal{E}}{2}\left(l+\frac{1}{2}\right), \qquad l = 0, 1, 2, \ldots. \tag{2}$$

Here, $\mathrm{H}_l(z)$ are the Hermite functions [10] and we have introduced the length scale $a = \sqrt{\frac{\hbar}{m\omega}}$ and the energy scale $\mathcal{E} = 2\hbar\omega = 2\frac{\hbar^2}{ma^2}$ (the unusual factor 2 is for our later convenience). The Hermite functions are even functions for even $l = 2k$ and odd functions for odd $l = 2k+1$, and fulfil

$$\mathrm{H}_{2k}(0) = (-1)^k\frac{(2k)!}{k!}, \qquad \mathrm{H}'_{2k+1}(0) = 2(2k+1)\mathrm{H}_{2k}(0). \tag{3}$$

Now let us divide the line into two by inserting an infinitely thin wall at $x = 0$ and consider its consequence in one of the half lines, say, the positive one. If the boundary condition on the wavefunctions at the wall is the Dirichlet condition, then for the particle confined in the positive half line, we have only the odd eigenfunctions, that is,

$$\varphi_k^{(\mathrm{Dir})} = \sqrt{2}\,\phi_{2k+1}, \qquad E_k^{(\mathrm{Dir})} = \mathcal{E}_{2k+1}, \qquad k = 0, 1, \ldots, \tag{4}$$

where the factor $\sqrt{2}$ is required for the normalization in the half line. On the other hand, if it is the Neumann boundary condition, then we have only the even eigenfunctions:

$$\varphi_k^{(\mathrm{Neu})} = \sqrt{2}\,\phi_{2k}, \qquad E_k^{(\mathrm{Neu})} = \mathcal{E}_{2k}, \qquad k = 0, 1, \ldots \tag{5}$$

One may wonder if there exist eigenfunctions other than these (4) and (5) in our system, since after all our partition wall breaks the parity symmetry under $x \to -x$ forcing us to work in two half lines separately, and there seems no reason to consider only the standard eigenfunctions of the harmonic oscillator defined on the whole line with definite parities. However, this cannot be the case, because if $\psi_+(x)$ is any eigenfunction defined on the positive half line obeying, say, the Dirichlet condition at $x = 0$, then one can extend it to the whole line by

setting $\psi(x) = \psi_+(x)$ for $x \geqslant 0$ and $\psi(x) = -\psi_+(-x)$ for $x < 0$. The resultant function $\psi(x)$ is regular at $x = 0$ and satisfies equation (1) on the whole line and hence provides an eigenfunction with odd parity of the harmonic oscillator, implying that it should be one of the standard ones ϕ_{2k+1}. The case of the solutions with the Neumann condition can be argued similarly.

To proceed, consider a statistical system consisting of N mutually noninteracting identical particles in the harmonic potential in the half line at finite temperature T. For convenience, we introduce the dimensionless quantities

$$t = k_{\mathrm{B}}T/\mathcal{E}, \qquad b = 1/t, \tag{6}$$

with k_{B} being the Boltzmann constant, and write the energy eigenvalues as

$$E_k = \mathcal{E}e_k, \qquad \text{with} \quad e_k = (k+\sigma), \qquad k = 0, 1, \ldots, \tag{7}$$

where the constant σ is given, for the Dirichlet case and the Neumann case, by

$$\sigma^{(\mathrm{Dir})} = \tfrac{3}{4}, \qquad \sigma^{(\mathrm{Neu})} = \tfrac{1}{4}, \tag{8}$$

respectively. The statistical distributions of the particles then read

$$N_k = \frac{1}{\mathrm{e}^{\alpha+be_k} - \eta} = \frac{1}{\mathrm{e}^{(\alpha+b\sigma)+bk} - \eta}, \qquad \eta = \begin{cases} 1 & \text{bosons} \\ -1 & \text{fermions.} \end{cases} \tag{9}$$

At a given temperature, the chemical constant α is uniquely determined from the constraint $N = \sum_{k=0}^{\infty} N_k$. This implies that the combination $\alpha + b\sigma$ is uniquely determined by this constraint, from which we learn that the distributions are actually the same for both the Dirichlet and the Neumann boundary conditions, that is, $N_k^{(\mathrm{Dir})} = N_k^{(\mathrm{Neu})}$ for all k. This allows us to introduce

$$\tilde{\alpha} := \alpha^{(\mathrm{Dir})} + b\sigma^{(\mathrm{Dir})} = \alpha^{(\mathrm{Neu})} + b\sigma^{(\mathrm{Neu})}, \qquad N_k := N_k^{(\mathrm{Dir})} = N_k^{(\mathrm{Neu})} \tag{10}$$

to obtain the simpler expression

$$N_k = \frac{1}{\mathrm{e}^{\tilde{\alpha}+bk} - \eta} \qquad k = 0, 1, \ldots, \tag{11}$$

commonly used for the two boundary conditions. We also find from $1/N_k = \mathrm{e}^{\tilde{\alpha}+bk} - \eta$ and $b > 0$ that $1/N_0 < 1/N_1 < 1/N_2 < \cdots$, or $N_0 > N_1 > N_2 > \cdots$. Note that for bosons $\eta = 1$, the positivity of distributions $N_k > 0$ for all k implies $\tilde{\alpha} > 0$ at any temperature (where the case $k = 0$ gives the strongest condition). For fermions $\eta = -1$, no such restriction emerges and $\tilde{\alpha}$ can take any value in $(-\infty, \infty)$.

At this point, we mention that the sum over the levels k admits an exact resummation valid for $\tilde{\alpha} > 0$:

$$\begin{aligned} N &= \sum_{k=0}^{\infty} \frac{1}{\mathrm{e}^{\tilde{\alpha}+bk} - \eta} = \sum_{k=0}^{\infty} \frac{\mathrm{e}^{-(\tilde{\alpha}+bk)}}{1 - \eta\,\mathrm{e}^{-(\tilde{\alpha}+bk)}} = \eta \sum_{k=0}^{\infty} \frac{\eta\,\mathrm{e}^{-\tilde{\alpha}}\mathrm{e}^{-bk}}{1 - \eta\,\mathrm{e}^{-\tilde{\alpha}}\mathrm{e}^{-bk}} \\ &= \eta \sum_{k=0}^{\infty} \sum_{l=1}^{\infty} (\eta\,\mathrm{e}^{-\tilde{\alpha}}\,\mathrm{e}^{-bk})^l = \eta \sum_{l=1}^{\infty} (\eta\,\mathrm{e}^{-\tilde{\alpha}})^l \sum_{k=0}^{\infty} \mathrm{e}^{-bkl} = \eta \sum_{l=1}^{\infty} \frac{(\eta\,\mathrm{e}^{-\tilde{\alpha}})^l}{1 - \mathrm{e}^{-bl}}, \end{aligned} \tag{12}$$

where we have used $\eta^{-1} = \eta$. This resummation formula will be useful later.

2.2. The force difference

Let us now suppose that the wall inserted at $x = 0$ in the harmonic potential imposes the Dirichlet boundary condition on the left (negative) side and the Neumann boundary condition

on the right (positive) side. Due to the difference in the energy levels developed on the two sides of the wall, one expects that a net force, or statistical pressure, will emerge on the wall as a purely quantum effect deriving from the boundary conditions (see figure 2). Our aim is to evaluate this induced net force as a function of (rescaled) temperature t.

Before we proceed, we recall the fact that for the case of the infinite potential well [9], the force acting on the wall from each side of the half lines proves to be essentially the same as the one giving the average energy, $\bar{E} = \sum_{k=0}^{\infty} N_k E_k$. From this, the net force is obtained by the difference $\Delta\bar{E} = \bar{E}^{(\mathrm{Dir})} - \bar{E}^{(\mathrm{Neu})}$. For the harmonic oscillator, the difference in the average energy reads

$$\Delta\bar{E} = \sum_{k=0}^{\infty} N_k \big(E_k^{(\mathrm{Dir})} - E_k^{(\mathrm{Neu})}\big) = \frac{\mathcal{E}}{2} \sum_{k=0}^{\infty} N_k (\sigma^{(\mathrm{Dir})} - \sigma^{(\mathrm{Neu})}) = \frac{N\mathcal{E}}{2}, \tag{13}$$

which is temperature independent.

However, for the harmonic oscillator the average energy is no longer the same as the force. To see this, let us consider the contribution F for the total force coming from one single level E. Under a shift δx of the wall from the origin, the energy level will also change by δE, and from this the force is found by

$$F = -\lim_{\delta x \to 0} \frac{\delta E}{\delta x}. \tag{14}$$

The total net force can then be obtained by gathering the force difference ΔF_k for all k, which is the difference of the forces between the two sides of the wall arising from the two corresponding energy levels specified by the same integer k. Unfortunately, unlike the infinite well case, we do not have analytical solutions for the harmonic oscillator when the partition is displaced from the centre, and we are compelled to resort to some approximation scheme to evaluate the force (14).

At this point we recall that, mathematically speaking, the Hamiltonian operator H of our system has the infinity $x = \pm\infty$ as a limit-point singularity whereas the position of the wall is a regular endpoint, meaning that for any real eigenvalue E, there exists only one normalizable eigenfunction up to a phase factor. In more concrete terms, given an arbitrary E we have two independent solutions for the differential equation (1) but requirement of normalizability determines a particular linear combination of the two as a possible candidate for an eigenfunction. It qualifies as a true eigenfunction when the boundary condition at the partition is further met, which is attained by tuning E to be one of the particular set of real numbers which form the energy spectrum of the system. This heuristic picture of approaching eigenfunctions and eigenvalues suggests that, if the shift δx of the wall is sufficiently small, for a fixed (Dirichlet or Neumann) boundary condition the difference in the eigenfunctions should be small in the L^2 sense that their scalar product tends to 1 as $\delta x \to 0$, with the perturbed eigenvalue $\tilde{E}$ also being close to the unperturbed one E. Similarly, we expect that for a small variation δx the difference in the boundary values of the two wavefunctions or their derivatives—the former is nonvanishing for the Neumann case while the latter is nonvanishing for the Dirichlet case—remains small and in the same order $\mathcal{O}(\delta x)$ at most.

Now, we consider the identity valid for any two real and normalized eigenfunctions:

$$\begin{aligned}(E - \tilde{E})(\varphi_{\tilde{E}}, \varphi_E)_+ &= (\varphi_{\tilde{E}}, H\varphi_E)_+ - (H\varphi_{\tilde{E}}, \varphi_E)_+ \\ &= \frac{\hbar^2}{2m}[\varphi_{\tilde{E}}(0)\,\varphi'_E(0) - \varphi'_{\tilde{E}}(0)\,\varphi_E(0)],\end{aligned} \tag{15}$$

where $(\,\cdot\,,\,\cdot\,)_+$ denotes the scalar product on the positive half line, and the prime indicates the derivative with respect to x, e.g., $\varphi' = \frac{d}{dx}\varphi$. Specifically, for the Dirichlet case, we choose

in (15) an unperturbed Dirichlet eigenvalue $E_k^{(\mathrm{Dir})}$ and its eigenfunction $\varphi_k^{(\mathrm{Dir})}$ for E and φ_E, and the perturbed eigenvalue and eigenfunctions caused by the shift in the wall for E and φ_E, respectively. Based on our observations on the perturbed quantities, we find that formula (15) in the leading order of δx or of $\delta E = E - E_k^{(\mathrm{Dir})}$ yields

$$\delta E = E - E_k^{(\mathrm{Dir})} \approx -\frac{\hbar^2}{2m}\varphi_k^{(\mathrm{Dir})\prime}(0)\,\varphi_E(0), \tag{16}$$

or

$$\varphi_E(0) \approx -\frac{\delta E}{\frac{\hbar^2}{2m}\varphi_k^{(\mathrm{Dir})\prime}(0)}. \tag{17}$$

In parallel, our assumption ensures that

$$\varphi_E'(0) \approx \varphi_k^{(\mathrm{Dir})\prime}(0), \tag{18}$$

and that the Dirichlet condition is satisfied at the shifted wall $x = \delta x$:

$$0 = \varphi_E(\delta x) \approx \varphi_E(0) + \varphi_E'(0)\cdot\delta x, \tag{19}$$

from which we have

$$\left(\frac{\delta E}{\delta x}\right)_k^{(\mathrm{Dir})} \approx \frac{\hbar^2}{2m}\left[\varphi_k^{(\mathrm{Dir})\prime}(0)\right]^2. \tag{20}$$

Analogously, for the Neumann case, we have

$$\delta E = E - E_k^{(\mathrm{Neu})} \approx \frac{\hbar^2}{2m}\varphi_k^{(\mathrm{Neu})}(0)\,\varphi_E'(0), \tag{21}$$

or

$$\varphi_E'(0) \approx \frac{\delta E}{\frac{\hbar^2}{2m}\varphi_k^{(\mathrm{Neu})}(0)}. \tag{22}$$

Since φ_E is an eigenfunction, we find

$$\varphi_E''(0) = -\frac{2mE}{\hbar^2}\varphi_E(0) \approx -\frac{2mE_k^{(\mathrm{Neu})}}{\hbar^2}\varphi_k^{(\mathrm{Neu})}(0). \tag{23}$$

The Neumann condition is satisfied at $x = \delta x$ if

$$0 = \varphi_E'(\delta x) \approx \varphi_E'(0) + \varphi_E''(0)\cdot\delta x, \tag{24}$$

from which we obtain

$$\left(\frac{\delta E}{\delta x}\right)_k^{(\mathrm{Neu})} \approx E_k^{(\mathrm{Neu})}\left[\varphi_k^{(\mathrm{Neu})}(0)\right]^2. \tag{25}$$

Combining (20) and (25) together with (2) and (3), one can evaluate the contribution for the force difference coming from the kth level as

$$\begin{aligned}\Delta F_k &= \frac{\hbar^2}{2m}\left[\varphi_k^{(\mathrm{Dir})\prime}(0)\right]^2 - E_k^{(\mathrm{Neu})}\left[\varphi_k^{(\mathrm{Neu})}(0)\right]^2 \\ &= \frac{\hbar^2}{2ma^2}\frac{2}{\sqrt{\pi}}\frac{1}{2^{2k+1}(2k+1)!}\left[\mathrm{H}_{2k+1}'(0)\right]^2 - \mathcal{E}\left(k+\frac{1}{4}\right)\frac{2}{\sqrt{\pi}a}\frac{1}{2^{2k}(2k)!}\left[\mathrm{H}_{2k}(0)\right]^2 \\ &= \frac{\mathcal{E}}{2\sqrt{\pi}a}\frac{(2k)!}{2^{2k}(k!)^2}.\end{aligned}$$

The final expression shows that ΔF_k has a nontrivial k-dependence in contrast to the infinite well case [9] where it is simply proportional to k.

Table 1. Exact and approximate values for Δf_k, for $k = 0, 1, 2, 3$.

k	Δf_k	$\frac{1}{\sqrt{\pi k}}$	$\frac{1}{\sqrt{\pi k}}\left[1-\frac{1}{8k}\right]$	$\frac{1}{\sqrt{\pi\,(k+1/4)}}$
0	1			1.128 38
1	0.5	0.564 19	0.493 67	0.504 63
2	0.375	0.398 94	0.374 01	0.376 13
3	0.3125	0.325 74	0.312 16	0.312 96

In what follows, for brevity we shall use the dimensionless force difference

$$\Delta f_k := 2\sqrt{\pi}a\frac{\Delta F_k}{\mathcal{E}} = \frac{(2k)!}{2^{2k}(k!)^2}, \tag{26}$$

which has the first few values

$$\Delta f_0 = 1, \qquad \Delta f_1 = \tfrac{1}{2}, \qquad \Delta f_2 = \tfrac{3}{8}, \qquad \Delta f_3 = \tfrac{5}{16}. \tag{27}$$

Note that, in general, $\Delta f_k > \Delta f_{k+1}$ (since $\Delta f_{k+1}/\Delta f_k = (2k+1)/(2k+2) < 1$) and, consequently, $\Delta f_k \leqslant 1$. To see how it behaves for large k, we may use the Stirling formula[3]

$$n! = \left(\frac{n}{e}\right)^n \sqrt{2\pi n}\left[1+\frac{1}{12n}+\mathcal{O}\left(\frac{1}{n^2}\right)\right] \tag{28}$$

to obtain

$$\frac{(2k)!}{2^{2k}(k!)^2} = \frac{1}{\sqrt{\pi k}}\left[1-\frac{1}{8k}+\mathcal{O}\left(\frac{1}{k^2}\right)\right], \tag{29}$$

which provides a sufficiently good approximation already at $k = 1$, and improves quickly for larger k. One can also observe that the 'rearranged' approximation

$$\Delta f_k \approx \frac{1}{\sqrt{\pi\,(k+1/4)}} \tag{30}$$

is similarly good as (29), and can be used for $k = 0$ as well (see table 1).

The total force difference (the net force) is then given by

$$\Delta f = \sum_{k=0}^{\infty} N_k\,\Delta f_k = \sum_{k=0}^{\infty}\frac{(2k)!}{2^{2k}(k!)^2}\frac{1}{\mathrm{e}^{\tilde{\alpha}+bk}-\eta}. \tag{31}$$

Now, using the resummation formula analogous to (12) together with the fact that a sum of the form

$$\sum_{k=0}^{\infty}\frac{(2k)!}{2^{2k}(k!)^2}\,q^k = \sum_{k=0}^{\infty}\binom{2k}{k}\left(\frac{q}{4}\right)^k \tag{32}$$

is actually the Taylor expansion of $1/\sqrt{1-q}$ for $|q| < 1$, we finally arrive at the convenient analytical expression of the net force:

$$\Delta f = \eta\sum_{l=1}^{\infty}(\eta\,\mathrm{e}^{-\tilde{\alpha}})^l\sum_{k=0}^{\infty}\frac{(2k)!}{2^{2k}(k!)^2}\mathrm{e}^{-bkl} = \eta\sum_{l=1}^{\infty}\frac{(\eta\,\mathrm{e}^{-\tilde{\alpha}})^l}{\sqrt{1-\mathrm{e}^{-bl}}}. \tag{33}$$

We mention that the inequality $\Delta f_k \leqslant 1$ noted earlier implies

$$\Delta f = \sum_{k=0}^{\infty} N_k\,\Delta f_k \leqslant \sum_{k=0}^{\infty} N_k = N. \tag{34}$$

[3] See, for instance, http://mathworld.wolfram.com/StirlingsApproximation.html. This also presents two strict inequalities, where the lower estimate and the higher one differ only in the sub-subleading order of $1/n$, which may be useful for proving strict inequalities, both for controlling numerical errors and for analytical strict bounds.

Clearly, this inequality (34) is expected to be close to the equality for low temperatures but it will become loose as temperature increases where the energy levels of higher k are excited with increasing probability. This way we can expect that the net force decreases as temperature increases. One can also obtain an improved inequality utilizing the closer details $\Delta f_0 = 1$ and $\Delta f_k \leqslant 1/2$ for $k > 0$, that is,

$$\Delta f = \sum_{k=0}^{\infty} N_k \, \Delta f_k = N - \sum_{k=1}^{\infty} N_k (1 - \Delta f_k) \leqslant N - \sum_{k=1}^{\infty} N_k \cdot 1/2 = (N + N_0)/2. \tag{35}$$

We have furnished analytical approximations for the net force which form our basis for studying the temperature dependence of the force on the partition wall. We stress that, unlike the case of the potential well, we further need to improve the approximations to obtain results comparable to numerical computations. This is required by the nontrivial level dependence (31) of the force in the harmonic case, and below we shall establish independent approaches to deal with infinite sums which are appropriate for three different temperature (high, low and medium) regimes.

3. The high-temperature regime

We now analyse the behaviour of the net force when the temperature is sufficiently high $t \gg 1$ or $b \ll 1$ (recall that $t = 1/b$ is the rescaled dimensionless temperature in (6)), where we are allowed to take $\tilde{\alpha} > 0$. One can then approximate formula (12) as

$$N = \eta \sum_{l=1}^{\infty} \frac{(\eta \, \mathrm{e}^{-\tilde{\alpha}})^l}{1 - \mathrm{e}^{-bl}} \approx \eta \sum_{l=1}^{\infty} \frac{(\eta \, \mathrm{e}^{-\tilde{\alpha}})^l}{bl}. \tag{36}$$

This approximation is certainly good for the terms $l \ll t$, but if we assume the condition $\mathrm{e}^{-\tilde{\alpha}} \ll 1$ (which is stronger than $\tilde{\alpha} > 0$) for which higher l terms in the sum (36) are suppressed, then we can rewrite (36) and perform the summation in a closed form as

$$\eta \frac{N}{t} \approx \sum_{l=1}^{\infty} \frac{(\eta \, \mathrm{e}^{-\tilde{\alpha}})^l}{l} = \ln \frac{1}{1 - \eta \, \mathrm{e}^{-\tilde{\alpha}}}, \tag{37}$$

which implies

$$\mathrm{e}^{-\tilde{\alpha}} \approx \eta \big(1 - \mathrm{e}^{-\eta \frac{N}{t}}\big) = \frac{N}{t} - \frac{\eta}{2} \left(\frac{N}{t}\right)^2 + \frac{1}{6} \left(\frac{N}{t}\right)^3 + \mathcal{O}\left(\left(\frac{N}{t}\right)^4\right). \tag{38}$$

We can see from this outcome that for sufficiently high temperatures $t \gg N$ our approximation is indeed consistent with $\mathrm{e}^{-\tilde{\alpha}} \ll 1$, suggesting that a valid approximation for $\tilde{\alpha}(t)$ can be obtained at least for t with $t \gg N$. Based on this observation, we shall define the high-temperature regime of the system by the condition $t \gg N$. Notably, here $\tilde{\alpha}$ depends on t and N only through the combination t/N.

Similarly, we can also approximate the net force (33) as

$$\Delta f = \eta \sum_{l=1}^{\infty} \frac{(\eta \, \mathrm{e}^{-\tilde{\alpha}})^l}{\sqrt{1 - \mathrm{e}^{-bl}}} \approx \eta \sum_{l=1}^{\infty} \frac{(\eta \, \mathrm{e}^{-\tilde{\alpha}})^l}{\sqrt{bl}} = \eta \sqrt{N} \left(\frac{t}{N}\right)^{\frac{1}{2}} \sum_{l=1}^{\infty} \frac{(\eta \, \mathrm{e}^{-\tilde{\alpha}})^l}{\sqrt{l}}. \tag{39}$$

Inserting the expansion (38), we find

$$\Delta f \approx \sqrt{N} \left(\frac{N}{t}\right)^{\frac{1}{2}} \left[1 + \eta \, c_1 \frac{N}{t} + c_2 \left(\frac{N}{t}\right)^2 + \eta \, c_3 \left(\frac{N}{t}\right)^3 + \mathcal{O}\left(\left(\frac{N}{t}\right)^4\right)\right], \tag{40}$$

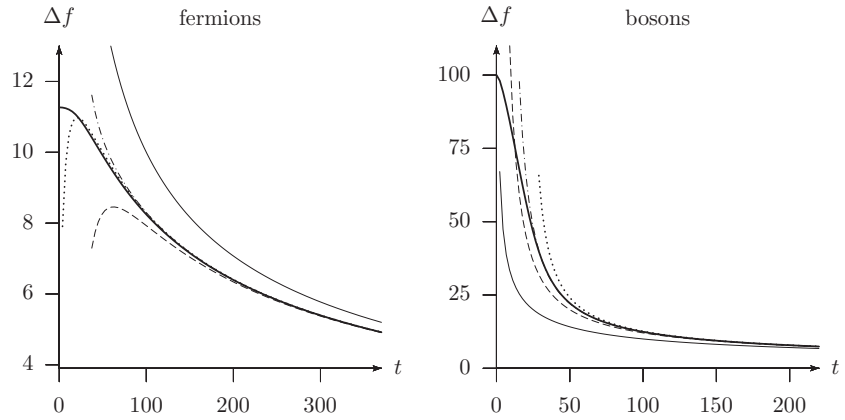

Figure 3. High-temperature approximations for Δf, for fermions (left) and bosons (right), $N = 100$. Thick solid line: the numerical result. Thin solid line: the expansion (40) truncated to one term. Dashed line: truncation to two terms. Dash-dotted line: truncation to three terms. Dotted line: (43).

with the coefficients

$$c_1 = \frac{\sqrt{2}-1}{2}, \qquad c_2 = \frac{1-3\sqrt{2}+2\sqrt{3}}{6}, \qquad c_3 = \frac{11+7\sqrt{2}-12\sqrt{3}}{24}. \tag{41}$$

Their numerical values are estimated as

$$c_1 \approx 0.207, \qquad c_2 \approx 0.0369, \qquad c_3 \approx 0.004\,79. \tag{42}$$

The analytical results, together with those improved below, are depicted in figure 3 along with the numerical ones. There we find that, for both the fermionic and the bosonic cases, the net force is a monotonically decreasing function in the high-temperature regime and vanishes in the limit $t \to \infty$. In fact, expression (40) shows that it decreases according to $1/\sqrt{t}$ asymptotically as $t \to \infty$ with the common order N. This outcome is in sharp contrast to the infinite well case [9] where the force $\Delta f(t)$ diverges according to $\sqrt{t}$ for both fermions and bosons (see figure 4).

It is worth noting that this high-temperature expansion can be made applicable even for medium temperatures if we modify it slightly by adopting the Padé approximant form [11] to regularize its diverging behaviour for $t \to 0$. Explicitly, we may take

$$\Delta f \approx \sqrt{N}\frac{\left(\frac{N}{t}\right)^{\frac{1}{2}}}{1-\eta\frac{\sqrt{2}-1}{2}\frac{N}{t}}, \qquad \text{or} \qquad \Delta f \approx \sqrt{N}\frac{\left(\frac{t}{N}\right)^{\frac{1}{2}}}{\frac{t}{N}-\eta\frac{\sqrt{2}-1}{2}} \tag{43}$$

both of which admit the expansion (40) but with slightly modified coefficients:

$$c_1 \approx 0.207, \qquad c_2 \approx 0.0429, \qquad c_3 \approx 0.008\,88. \tag{44}$$

We note that the regularized formula (43) reproduces the analytical approximation (40) quite well up to the third term (the fourth also not being very different). However, for bosons the attempt to regularize at $t = 0$ fails because (43) diverges at a certain positive medium temperature value, i.e. $\frac{t}{N} = \frac{\sqrt{2}-1}{2}$, and this also ruins improvement in precision. For fermions, in contrast, the approximation is indeed valid up to fairly low temperatures. It is also important to observe from the result (40) that, similarly to $\tilde{\alpha}$, the net force $\Delta f/\sqrt{N}$ also depends on t and N only through the combination t/N in the high-temperature regime.

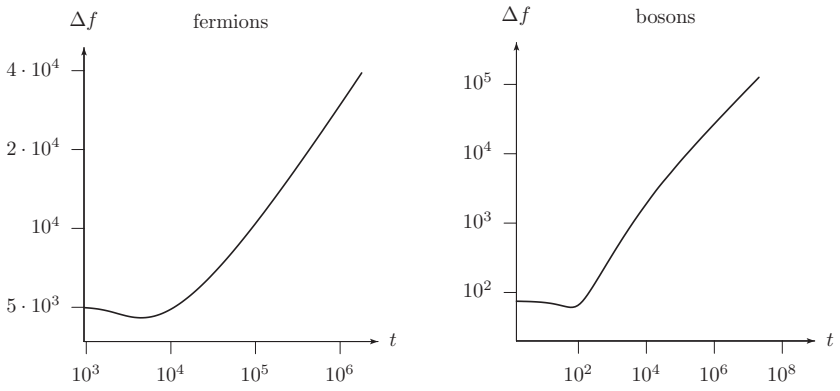

Figure 4. Numerical results of the net force Δf in the infinite well case; for fermions (left) and bosons (right), at $N = 100$. The net force diverges as $t \to \infty$ according to $\sqrt{t}$ for both fermions and bosons [9].

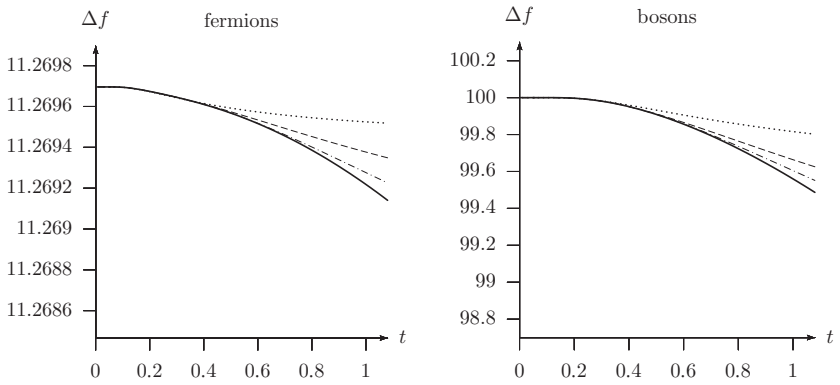

Figure 5. Low-temperature approximations for Δf for fermions (left) and bosons (right), $N = 100$. Thick solid line: the numerical result. Dotted line: the fermionic expansion (53) up to the term $\mathrm{e}^{-\frac{b}{2}}$, respectively the bosonic expansion (58) up to the term e^{-b}. Dashed line: terms up to $\mathrm{e}^{-\frac{3b}{2}}$, resp. e^{-2b}. Dash-dotted line: terms up to $\mathrm{e}^{-\frac{5b}{2}}$, resp. e^{-3b}.

In passing, we provide a technical remark that, if one wishes to improve the approximations (36) and (39) to curb the error caused by the replacement $1 - \mathrm{e}^{-bl} = bl + \mathcal{O}((bl)^2) \approx bl$ used above, one may instead use $\mathrm{e}^{\frac{bl}{2}} - \mathrm{e}^{-\frac{bl}{2}} = bl + \mathcal{O}((bl)^3) \approx bl$ (which is more precise by one order) to obtain

$$\sum_{l=1}^{\infty} \frac{(\eta\, \mathrm{e}^{-\tilde{\alpha}})^l}{1 - \mathrm{e}^{-bl}} \approx \sum_{l=1}^{\infty} \frac{\left(\eta\, \mathrm{e}^{-\tilde{\alpha}+\frac{b}{2}}\right)^l}{bl}, \qquad \sum_{l=1}^{\infty} \frac{(\eta\, \mathrm{e}^{-\tilde{\alpha}})^l}{\sqrt{1 - \mathrm{e}^{-bl}}} \approx \sum_{l=1}^{\infty} \frac{\left(\eta\, \mathrm{e}^{-\tilde{\alpha}+\frac{b}{4}}\right)^l}{\sqrt{bl}}, \tag{45}$$

respectively. Although the acquired improvements in $\tilde{\alpha}$ and in Δf are of the order of $1/t$ and hence insignificant for $N \to \infty$, they may become significant for $N \sim 100$.

4. The low-temperature regime

Next we turn our attention to the net force when the temperature is sufficiently low. In this regime we need to develop our approximation depending the statistics of the particles, and below we present our arguments for fermions and bosons, separately.

4.1. Fermions at low temperature

Note first that, for the fermionic case $\eta = -1$, the particle distribution at $t = 0$ becomes

$$N_0 = N_1 = \cdots = N_{N-1} = 1, \qquad N_N = N_{N+1} = \cdots = 0, \tag{46}$$

for which $\tilde{\alpha}$ is, so to say, $-\infty$. The net force is then

$$\Delta f(0) = \sum_{k=0}^{N-1} \Delta f_k = \sum_{k=0}^{N-1} \frac{(2k)!}{2^{2k}(k!)^2} = \frac{2N(2N)!}{2^{2N}N!^2} = 2\sqrt{\frac{N}{\pi}}\left[1 - \frac{1}{8N} + \mathcal{O}\left(\frac{1}{N^2}\right)\right], \tag{47}$$

where the exact result is, at the last step, approximated for large N using the Stirling formula. Observe that the limiting value $\Delta f(0)$ is of the order $\sqrt{N}$ for large N.

For a slightly higher temperature $t > 0$, we may assume that the distribution differs from (46) only at N_{N-1} and N_N. Then $\sum_{k=0}^{\infty} N_k = N$ implies $N_{N-1} + N_N = 1$, which can be exploited as

$$\frac{1}{\mathrm{e}^{\tilde{\alpha}+bN}+1} = N_N = 1 - N_{N-1} = 1 - \frac{1}{\mathrm{e}^{\tilde{\alpha}+b(N-1)}+1} = \frac{\mathrm{e}^{\tilde{\alpha}+b(N-1)}}{\mathrm{e}^{\tilde{\alpha}+b(N-1)}+1} \tag{48}$$

which is equivalent to

$$\tilde{\alpha} = -b\big(N - \tfrac{1}{2}\big), \tag{49}$$

in this approximation.

For the net force, we can use the same approximate distribution, but we may further suppose that (49) is a good approximation even when more than two levels—let their number be denoted by $2J$, still assuming $2J \ll 2N$—get nontrivially occupied. Then the net force Δf will differ from the zero temperature value $\Delta f(0)$ as

$$\begin{aligned}
\Delta f - \Delta f(0) &= \sum_{k=0}^{\infty} \Delta f_k N_k - \sum_{k=0}^{N-1} \Delta f_k = -\sum_{k=0}^{N-1} \Delta f_k\,(1 - N_k) + \sum_{k=N}^{\infty} \Delta f_k N_k \\
&\approx -\sum_{k=N-J}^{N-1} \Delta f_k (1 - N_k) + \sum_{k=N}^{N+J-1} \Delta f_k N_k \\
&= -\sum_{j=1}^{J} \Delta f_{N-j} \left(1 - \frac{1}{\mathrm{e}^{b(\frac{1}{2}-j)}+1}\right) + \sum_{j=1}^{J} \Delta f_{N-1+j} \frac{1}{\mathrm{e}^{b(j-\frac{1}{2})}+1}.
\end{aligned} \tag{50}$$

This can be further approximated by using (30) as

$$\Delta f - \Delta f(0) = \sum_{j=1}^{J} \frac{\Delta f_{N-1+j} - \Delta f_{N-j}}{\mathrm{e}^{b(j-\frac{1}{2})}+1} \approx \sum_{j=1}^{J} \frac{\frac{1}{2\sqrt{\pi}N^{\frac{3}{2}}}(1-2j)}{\mathrm{e}^{b(j-\frac{1}{2})}+1}, \tag{51}$$

from which we obtain

$$\Delta f \approx \Delta f(0) - \frac{1}{2\sqrt{\pi}N^{\frac{3}{2}}}\left[\frac{1}{\mathrm{e}^{\frac{b}{2}}+1} + \frac{3}{\mathrm{e}^{\frac{3b}{2}}+1} + \cdots\right], \tag{52}$$

on account of $j \leqslant J \ll N$. As an expansion in terms of $\mathrm{e}^{-\frac{b}{2}}$, (52) turns into

$$\Delta f \approx \Delta f(0) - \frac{1}{2\sqrt{\pi}N^{\frac{3}{2}}}\left[\mathrm{e}^{-\frac{b}{2}} - \mathrm{e}^{-b} + 4\,\mathrm{e}^{-\frac{3b}{2}} - \mathrm{e}^{-2b} + 6\,\mathrm{e}^{-\frac{5b}{2}} + \cdots\right]. \tag{53}$$

This result shows that, relative to the zero temperature value whose leading order is $\sqrt{N}$ (see (47)), the temperature dependence of the net force Δf starts at the order of $1/N^2$. As a result, a noticeable deviation from $\Delta f(0)$ can be expected only for $t \gg 1$.

4.2. Bosons at low temperature

For the bosons $\eta = 1$, we know that at $t = 0$, the distribution is given by $N_0 = N$ and $N_k = 0$ for $k > 0$, and hence $N_0 = 1/\mathrm{e}^{\tilde{\alpha}} - 1 = N$. This implies

$$\tilde{\alpha} = \ln\left(1 + \frac{1}{N}\right) \approx \frac{1}{N}. \tag{54}$$

The net force at $t = 0$ is thus

$$\Delta f(0) = \Delta f_0\, N_0 = N. \tag{55}$$

When the temperature grows from zero, $\tilde{\alpha}$ is expected to change continuously with t, and we may define the low-temperature regime for bosons by $\tilde{\alpha} < 1$ so that $\mathrm{e}^{-\tilde{\alpha}} \approx 1$ along with $t < 1$. Then we can write for $k > 0$:

$$N_k = \frac{1}{\mathrm{e}^{\tilde{\alpha}+bk} - 1} = \frac{\mathrm{e}^{-\tilde{\alpha}-bk}}{1 - \mathrm{e}^{-\tilde{\alpha}-bk}} \approx \mathrm{e}^{-bk} + \mathrm{e}^{-2bk} + \mathrm{e}^{-3bk} + \cdots, \tag{56}$$

where one can expect that, when n is high enough so that $\mathrm{e}^{-n\tilde{\alpha}}$ ceases to be near 1, the factor e^{-nbk} appearing in the nth term becomes very small. Consequently, in this low-temperature regime, we have

$$N_0 = N - \sum_{k=1}^{\infty} N_k \approx N - \mathrm{e}^{-b} - 2\,\mathrm{e}^{-2b} - 2\,\mathrm{e}^{-3b} - \cdots. \tag{57}$$

Plugging (56) and (57) into (31) and arranging terms according to the powers of e^{-b}, we find

$$\Delta f \approx N - \tfrac{1}{2}\,\mathrm{e}^{-b} - \tfrac{9}{8}\,\mathrm{e}^{-2b} - \tfrac{19}{16}\,\mathrm{e}^{-3b} + \cdots. \tag{58}$$

We can see that, in the bosonic case, the temperature dependence of Δf begins at the order of $1/N$ with respect to the zero temperature value.

5. The medium-temperature regime

We have so far gained reasonably good approximations of the net force for high- and low-temperature regimes. In this section we wish to study the temperature regime between the two, hoping to find some approximation to interpolate the previous two. Again, we consider the cases of fermions and bosons, separately.

5.1. Fermions at medium temperature

We have seen for fermions that, at $t \sim 1$, the net force $\Delta f(t)$ is still very close to $\Delta f(0)$. For a noticeable departure from $\Delta f(0)$, one needs to go above $t \sim 1$, presumably to $t \gg 1$ (or $b \ll 1$), in which case the sum (9) can be approximated by the integral

$$N = \sum_{k=0}^{\infty} \frac{1}{\mathrm{e}^{\tilde{\alpha}+bk} - 1} = \frac{1}{\Delta y}\sum_{k=0}^{\infty} \frac{\Delta y}{\mathrm{e}^{\tilde{\alpha}+y_k} + 1} \approx \frac{1}{\Delta y}\int_0^{\infty} \frac{\mathrm{d}y}{\mathrm{e}^{\tilde{\alpha}+y} + 1} = \frac{1}{b}\ln(1 + \mathrm{e}^{-\tilde{\alpha}}), \tag{59}$$

where we have used $y_k := bk$, $\Delta y := y_{k+1} - y_k = b$. This implies

$$\mathrm{e}^{-\tilde{\alpha}} \approx \mathrm{e}^{\frac{N}{t}} - 1, \tag{60}$$

which is just (38), showing that the formula remains valid for medium temperatures as well.

Precise evaluation of $\mathrm{e}^{-\tilde{\alpha}}$ is particularly important in this temperature regime, because the final outcome of the net force Δf is extremely sensitive to the variation of $\mathrm{e}^{-\tilde{\alpha}}$. For this reason, it is worthy to consider an improved approximation obtained from the fact that, for 'well-behaved' functions $g(y)$ in $[y_0, \infty)$ with $\lim_{y\to\infty} g(y) = 0$, the trapezoid approximation of integrals yields

$$\sum_{k=0}^{\infty} g(y_k) \approx \frac{g(y_0)}{2} + \frac{1}{\Delta y}\int_{y_0}^{\infty} g(y)\,\mathrm{d}y, \tag{61}$$

which is better than that acting in (59) by one order. As a result, one finds that the first correction term on the rhs of (61) improves (60) to

$$\mathrm{e}^{-\tilde{\alpha}} \approx \mathrm{e}^{\frac{N-N_0/2}{t}} - 1. \tag{62}$$

This formula (62) reduces to (60) for high temperatures where $N_0 \ll 1 \ll N$, and to (49) for low temperatures where $N_0 \approx 1$ and the second term in (62) is negligible compared to the first term. Note that the presence of $N_0 \leqslant 1$ in the improvement is not insignificant, since at low temperatures $\mathrm{e}^{\frac{N-1/2}{t}}$ can be significantly different from $\mathrm{e}^{\frac{N}{t}}$ on account of the ratio being $\mathrm{e}^{\frac{1}{2t}} \not\approx 1$. It also suggests that the deviation of N_0 from its zero temperature value 1 may become important for medium temperatures, too.

To acquire a meaningful formula between the low- and high-temperature regimes, we can use (62) where the presence of N_0 is expected to provide sensitivity to the low-temperature regime, with the approximation that N_0 is given by its high-temperature value from (60), $N_0 \approx 1 - \mathrm{e}^{-N/t}$, that is,

$$\mathrm{e}^{-\tilde{\alpha}} \approx \mathrm{e}^{(N-\frac{1-\mathrm{e}^{-N/t}}{2})/t} - 1. \tag{63}$$

As can be seen in figure 6(*a*), this approximation formula for $\mathrm{e}^{-\tilde{\alpha}}$ holds actually very well on the whole temperature regime. Similar improvement for the net force is a bit harder to achieve. Here, we will restrict ourselves only to leading-order approximations, and proceed as

$$\begin{aligned}\Delta f &\approx \sum_{k=0}^{\infty} \frac{1}{\sqrt{\pi\,(k+1/4)}}\frac{1}{\mathrm{e}^{\tilde{\alpha}+bk}-1} = \frac{1}{\Delta y}\sqrt{\frac{b}{\pi}}\sum_{k=0}^{\infty}\frac{\Delta y}{\sqrt{y_k+b/4}(\mathrm{e}^{\tilde{\alpha}+y_k}+1)} \\ &\approx \frac{1}{\sqrt{\pi b}}\int_0^{\infty}\frac{\mathrm{d}y}{\sqrt{y+b/4}(\mathrm{e}^{\tilde{\alpha}+y}+1)},\end{aligned} \tag{64}$$

using (30) again, and considering b small enough. Introducing $z := \sqrt{y+b/4}$, we can rewrite it as

$$\Delta f \approx \frac{2}{\sqrt{\pi b}}\int_{\sqrt{b/4}}^{\infty}\frac{\mathrm{d}z}{\mathrm{e}^{\tilde{\alpha}-b/4+z^2}+1} \approx \frac{2}{\sqrt{\pi b}}\int_0^{\infty}\frac{\mathrm{d}z}{\mathrm{e}^{\tilde{\alpha}+z^2}+1}. \tag{65}$$

For negative $\tilde{\alpha}$, the resulting integral can be approximated by an asymptotic series [12, 13] to obtain

$$\Delta f \approx \frac{2}{\sqrt{\pi b}}\sqrt{-\tilde{\alpha}}\left[1 - \frac{\pi^2}{24}\frac{1}{\tilde{\alpha}^2} - \frac{7\pi^4}{384}\frac{1}{\tilde{\alpha}^4} + \mathcal{O}\left(\frac{1}{\tilde{\alpha}^6}\right)\right]. \tag{66}$$

The divergence of the formula for $\tilde{\alpha} \to 0$ may be dealt with by adopting the Padé form

$$\Delta f \approx \frac{2}{\sqrt{\pi b}}\,\frac{\sqrt{-\tilde{\alpha}}}{1 + \frac{\pi^2}{24}\frac{1}{\tilde{\alpha}^2} + \frac{23\pi^4}{1152}\frac{1}{\tilde{\alpha}^4}}, \tag{67}$$

which improves its validity towards $\tilde{\alpha} \to 0$,

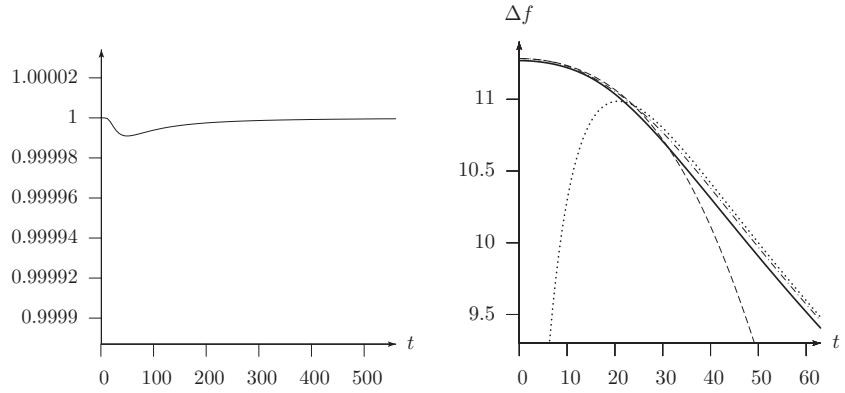

Figure 6. Fermions, $N = 100$. (a) The ratio of the approximate $e^{-\tilde{\alpha}}$ provided by (63) to the numerically determined $e^{-\tilde{\alpha}}$. The largest relative error is 10^{-5} along the whole temperature region $0 < t < \infty$. (b) The net force Δf. Solid line: the numerical result. Dashed line: the low+medium-temperature approximation (68). Dotted line: the high-temperature approximation (43). Dash-dotted line: the interpolating curve (69) with the choices mentioned in the text.

In the medium-temperature regime, one may expect that the temperature is low enough for the second term of (62) to be omitted, while it is high enough for $N_0/2$ to be omitted. If this is the case, one can simplify (62) to $e^{-\tilde{\alpha}} \approx e^{\frac{N}{t}}$ or $-\tilde{\alpha} \approx \frac{N}{t}$, which can be inserted into (67) to obtain

$$\Delta f \approx \sqrt{N}\,\frac{\frac{2}{\sqrt{\pi}}}{1+\frac{\pi^2}{24}\left(\frac{t}{N}\right)^2+\frac{23\pi^4}{1152}\left(\frac{t}{N}\right)^4}\,. \tag{68}$$

Note that this formula takes care of the zero temperature value $\Delta f(0)$ correctly, and that, similarly to (43), the ratio $\Delta f/\sqrt{N}$ is again a function of t and N only through the combination t/N.

Plotting the low+medium-temperature curve (68), and the high-temperature one (43), we find that the two together actually cover the whole temperature range (see figure 6(b)). From a technical viewpoint, we may find it convenient to introduce an interpolating function for the two curves connecting smoothly. This can be accomplished by using, for example, the scheme

$$g_{\rm intp}(x) := \frac{1\cdot g_1(x)+(x/x_*)^p\cdot g_2(x)}{1+(x/x_*)^p}, \tag{69}$$

where $g_{\rm intp}(x)$ gives the interpolating function of the two curves described by $g_1(x)$ and $g_2(x)$. The interpolating point x_* may be chosen as the value where $g_1(x_*) = g_2(x_*)$ holds, which ensures that at x_* the weights $\frac{1}{1+(x/x_*)^p}$ and $\frac{(x/x_*)^p}{1+(x/x_*)^p}$ are equal irrespective of the value of p.

In our case, we have $x = t/N$ and choose the function Δf in (68) for g_1 and the function Δf in (43) for g_2. Then the numerically determined value of the interpolating point for $N = 100$ is found to be $(t/N)_* = 0.237\,845$. As for p, we know that (68) is precise up to the order of $(t/N)^5$, and if we maintain this then we find that the smallest choice is $p = 5$. Since this choice does not disturb the high-temperature expansion either, we may propose the resultant interpolating formula $g_{\rm intp}$ in (69) as the net force covering the whole temperature region. Figure 6(b) shows that this single formula reproduces the precise curve (obtained numerically) very well. Note that this interpolating procedure is actually independent of N, since, for all Ns, it involves the same functions (low- and high-temperature approximants of $\Delta f/\sqrt{N}$) of the identical variable t/N.

5.2. Bosons at medium temperature

This time we are again allowed to replace the sums by integrals with the approximation (61). Since for low temperatures N_0 is much larger than higher N_k, we preserve its discrete value and introduce the continuous variable only above $k = 1$. This gives

$$N = N_0 + \sum_{k=1}^{\infty} N_k \approx N_0 + \frac{N_1}{2} + \frac{1}{\Delta y}\int_{y_1}^{\infty} \frac{\mathrm{d}y}{\mathrm{e}^{\tilde{\alpha}+y}-1}$$
$$= \frac{1}{\mathrm{e}^{\tilde{\alpha}}-1} + \frac{\frac{1}{2}}{\mathrm{e}^{\tilde{\alpha}+b}-1} + \frac{1}{b}\ln\frac{1}{1-\mathrm{e}^{-\tilde{\alpha}-b}}\,. \tag{70}$$

For the medium-temperature regime, we find it reasonable to assume that it is characterized by $\tilde{\alpha} \ll 1$ and $t \gg 1$. Under this, one may simplify the outcome by putting $\tilde{\alpha} = \frac{b}{4}$ in all terms except the first in expansion (70) (the advantage of the specific value $\frac{b}{4}$ will turn out soon), since by far the first term $N_0 = \frac{1}{\mathrm{e}^{\tilde{\alpha}}-1}$ is the most sensitive term for the change of $\tilde{\alpha}$ on the scale of b or below. In this approximation, (70) leads to

$$N_0 = \frac{1}{\mathrm{e}^{\tilde{\alpha}}-1} \approx N - \frac{\frac{1}{2}}{\mathrm{e}^{\frac{5b}{4}}-1} - \frac{1}{b}\ln\frac{1}{1-\mathrm{e}^{-\frac{5b}{4}}} \approx N - \frac{2}{5}t - t\ln\frac{4}{5}t\,. \tag{71}$$

The net force can also be evaluated by treating the sum analogously as

$$\Delta f = N_0 + \sum_{k=1}^{\infty} \Delta f_k N_k \approx N_0 + \frac{\Delta f_1 N_1}{2} + \frac{2}{\sqrt{\pi b}}\int_{\sqrt{\frac{5b}{4}}}^{\infty} \frac{\mathrm{d}z}{\mathrm{e}^{z^2}-1},$$
$$\approx N_0 + \frac{1}{2}\frac{\frac{1}{2}}{\mathrm{e}^{\frac{5b}{4}}-1} + \frac{2}{\sqrt{\pi b}}\int_{\sqrt{\frac{5b}{4}}}^{\infty}\left[\frac{1}{z^2}-\frac{1}{2}\right]\mathrm{d}z, \tag{72}$$

where we have gone through steps similar to (65) and introduced an asymptotic expansion for the integrand to improve it in the dominant region. Note that the choice $\tilde{\alpha} = \frac{b}{4}$ has made this integral $\tilde{\alpha}$-independent.

Actually, the approximation of the integrand with the asymptotic expansion becomes better if we keep only the part of the integral where the approximated integrand is positive. Because of this, we use

$$\int_{\sqrt{\frac{5b}{4}}}^{\sqrt{2}}\left[\frac{1}{z^2}-\frac{1}{2}\right]\mathrm{d}z = \sqrt{\frac{4}{5}t} - \sqrt{2} + \mathcal{O}(\sqrt{b}) \tag{73}$$

and (71) to evaluate (72) and find

$$\Delta f \approx N + \left[-\frac{2}{5} - \ln\frac{4}{5} + \frac{1}{5} + \frac{4}{\sqrt{5\pi}}\right]t - t\ln t + \sqrt{\frac{4}{5}t} - \sqrt{2}. \tag{74}$$

We may further consider some corrections for the expression to render it a little nicer without sacrificing its precision. This is done by omitting the last term $\sqrt{2}$ which is negligible compared to the first term N, which makes the $t = 0$ limiting value the exact value $\Delta f(0) = N$. We also replace the coefficient of t which is numerically 1.032 by 1 for simplicity. We then end up with

$$\Delta f \approx N + t - t\ln t + \sqrt{\tfrac{4}{5}t}. \tag{75}$$

As for lower temperatures the $\tilde{\alpha}$-dependence of the terms $k \geqslant 1$ is suppressed more, and since we could reach a formula that is precise even at $t = 0$, we may hope that, in spite of the assumption $\tilde{\alpha} \approx \frac{b}{4}$ made above, this formula (75) can be used even for the beginning part of the net force $\Delta f(t)$ including $t = 0$. Figure 7 shows that this is indeed the case.

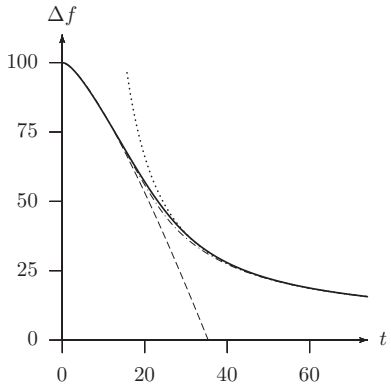

Figure 7. The net force Δf for bosons, $N = 100$. Solid line: the numerical result. Dashed line: the low+medium-temperature approximation (75). Dotted line: the high-temperature approximation (40). Dash-dotted line: the interpolating curve (69), for $t_* = 22.925$ and $p = 9$.

It is again possible to provide an interpolating formula between the low-temperature approximation and the high-temperature one based on formula (69) by choosing the functions (75) and (40) for g_1 and g_2, respectively. Note, however, that this time the two curves do not cross each other, and the interpolating point t_* may be chosen, e.g., as the location where the two functions differ the least. For example, for $N = 100$, this yields $t_* := 22.925$. In addition, the value of p can be chosen, for instance, by the requirement that the derivative of the interpolating function at $t = t_*$ be the same as that of the straight line that is the common tangent of the two curves to be connected. At $N = 100$, that common tangent straight line touches the low-temperature curve at the point [7.338, 88.46] and the high-temperature curve at [26.12, 45.66] in the coordinate plane of t and Δf. The slope of that straight line is -2.278, and this is to be put equal to the derivative of (69) at x_*, i.e. $\frac{\mathrm{d}g_{\mathrm{intp}}}{\mathrm{d}x}(x_*) = \frac{\mathrm{d}g_2}{\mathrm{d}x}(x_*) + \frac{p}{x_*}\frac{g_2(x_*)-g_1(x_*)}{4}$, where we have used $\frac{\mathrm{d}g_1}{\mathrm{d}x}(x_*) = \frac{\mathrm{d}g_2}{\mathrm{d}x}(x_*)$ which comes from the definition of x_* being the location where the difference is minimal. From this we find $p = 8.641$. One can invent some other criteria as well, but our aim here is only to present a formula in which the transition between the two curves appears as smoothly as possible, yet sharply enough to keep both curves practically intact on the regions where they are supposed to be reliable.

Since the accuracy of the interpolation employed above is not very sensitive to the actual value of p, we may round it off to the nearest integer $p = 9$, say, for brevity. Figure 7 shows the resultant interpolating formula (69) with our choice of functions, which is almost indistinguishable from the numerical result. We should, however, keep in mind that for bosons the interpolation must be done N-dependently, because the scaling behaviour $\frac{\Delta f}{\sqrt{N}} = \frac{\Delta f}{\sqrt{N}}\left(\frac{t}{N}\right)$ seen at the high-temperature regime does not arise at the low-temperature regime. It also follows that a successful interpolation at some N does not necessarily ensure a success for an analogously carried out interpolation at another N.

6. Conclusion and discussions

In this paper, we studied the system of N particles confined in each of the two half lines separated by a partition wall at the centre of the harmonic oscillator potential. The partition is assumed to impose a set of distinct—the Dirichlet and the Neumann—boundary conditions

on the left and on the right, respectively. Due to the discordance in the energy levels in two sides of the partition, and also to the different distributions of particles on the energy levels at finite temperatures, an induced force emerges on the partition, as we have seen earlier on the partition in the infinite potential well.

We have evaluated the (dimensionless) net force $\Delta f(t)$ that arises on the wall both analytically and numerically as a function of (dimensionless) temperature t, and found that it exhibits a number of interesting behaviours characteristic to the harmonic potential. For instance, it has a non-vanishing limit $\Delta f(0)$ at the zero temperature limit, which is just N for bosons, while it is of the order of $\sqrt{N}$ for fermions. Note that in the case of the infinite potential well [9], the value $\Delta f(0)$ for fermions is proportional to N^2.

On the other hand, in the high-temperature regime, the force $\Delta f(t)$ scales linearly in N for both fermions and bosons. As temperature grows, it decreases according to $1/\sqrt{t}$ and eventually vanishes in the limit $t \to \infty$. This is in sharp contrast to the infinite potential well case where the force $\Delta f(t)$ diverges according to $\sqrt{t}$.

The medium-temperature regime is somewhat difficult to deal with, but we have succeeded to obtain, after a rather technical argument, an analytic approximation that accounts for the numerical results reasonably well for both fermions and bosons. Interpolation to the low- and high-temperature regimes can also be possible, and we presented a possible formula of the force covering the entire regime of temperature. Unlike the potential well case, the net force admits no minimum in the medium-temperature regime.

The characteristic scaling behaviours in the zero temperature limit $t \to 0$ can be understood heuristically. Namely, in the bosonic case, the force $\Delta f(0)$ comes entirely from the contribution of the ground level where all particles reside, and hence it is given by Δf_0 multiplied by the number N of the particles. In the fermionic case, on the other hand, the force $\Delta f(0)$ consists of the contributions of $\Delta f_k \approx (\pi k)^{-\frac{1}{2}}$ up to the Fermi level, yielding $\Delta f(0) \propto \sum_{k=1}^{N} k^{-\frac{1}{2}} \propto N^{\frac{1}{2}}$. This is to be compared to the infinite potential well case where we have $\Delta f_k \approx k$ and hence $\Delta f(0) \propto \sum_{k=1}^{N} k \propto N^2$.

In the high-temperature regime, it can also be argued that the steady decrease in the present harmonic potential case, rather than the increase to infinity observed in the potential well case, derives basically from the spectral structure of the harmonic system. That is, for higher n the energy level difference between the two half harmonic systems remains constant and does not give larger contributions, in contrast to the potential well case where the energy level difference becomes larger and eventually diverges for $n \to \infty$. In this respect, we recall the upper bound (34) for the force $\Delta f(t)$ whose decrease for higher t is already expected there as well. In physical terms, this is also understood from the infinite stretch of the harmonic potential where the higher energy states can spread more in space. As a result, the energy of the system becomes less sensitive to a shift of the partition at the centre, resulting in the decrease in the force for high temperatures.

What can we learn from the results obtained here for the harmonic system when combined with those obtained previously for the infinite potential well system? Suppose that a partition wall can actually be manufactured with the distinct set of boundary conditions assumed in this paper, and further that the induced force on the partition wall can be measured with sufficient accuracy. Then, one can estimate the profile of the potential in the neighbourhood of the partition wall by looking at the low-temperature behaviour of Δf, since the net force is sensitive to the spectral structure up to the Fermi level for fermions when the temperature is low. From the high-temperature behaviour of Δf, one can also obtain a crude picture of how the potential stretches in space further away from the wall. In addition, the characteristic scaling in the number N of particles in the zero temperature limit will reveal the statistics of

the particles contained around the wall. In short, such a nontrivial partition wall may be quite useful in probing the profile of the potential as well as the statistics of the particles involved. The present probe is still primitive to use for generic potentials, but it can be improved if we learn further the behaviours of the net force for other types of potentials in the high- and the low-temperature regimes along with the scaling property in the particle number.

Acknowledgments

This work has been supported in part by the Grant-in-Aid for Scientific Research (C), No. 20540391-H21, MEXT, Japan.

References

[1] Jackiw R 1984 *Relativity, Groups and Topology II* ed B S DeWitt and R Stora (Amsterdam: North-Holland)
[2] Reed M and Simon B 1975 *Methods of Modern Mathematical Physics II, Fourier Analysis, Self-Adjointness* (New York: Academic)
[3] Akhiezer N I and Glazman I M 1981 *Theory of Linear Operators in Hilbert Space* vol 2 (Boston: Pitman)
[4] Albeverio S, Gesztesy F, Høegh-Krohn R and Holden H 2004 *Solvable Models in Quantum Mechanics* 2nd edn (Providence, RI: AMS Chelsea Publishing)
[5] Fülöp T, Cheon T and Tsutsui I 2002 *Phys. Rev.* A **66** 052102
[6] Cheon T, Fülöp T and Tsutsui I 2001 *Ann. Phys.* **294** 1
[7] Tsutsui I, Fülöp T and Cheon T 2001 *J. Math. Phys.* **42** 5687
[8] Fülöp T and Tsutsui I 2000 *Phys. Lett.* A **264** 366
[9] Fülöp T and Tsutsui I 2007 *J. Phys. A: Math. Theor.* **40** 4585
[10] Abramowitz M and Stegun I A (eds) 1965 *Handbook of Mathematical Functions with Formulas, Graphs, and Mathematical Tables* (New York: Dover)
[11] Baker G A Jr and Graves-Morris P 1996 *Padé Approximants* (New York: Cambridge University Press)
[12] Greiner W, Neise L and Stöcker H 1995 *Thermodynamics and Statistical Mechanics* (New York: Springer)
[13] McDougall J and Stoner E C 1938 *Phil. Trans. R. Soc.* A **237** 67